Modeling and Simulation of the Thermal Runaway in Cylindrical 18650 Lithium-Ion Batteries

Andreas Melcher[*], Carlos Ziebert, Magnus Rohde, Boxia Lei, Hans Jürgen Seifert
Institute of Applied Materials - Applied Materials Physics, Karlsruhe Institute of Technology
*Corresponding author: Hermann-von-Helmholtz-Platz-1, Eggenstein-Leopoldshafen 76344, Germany,
Andreas.Melcher@kit.edu

Abstract: In this work the coupled electrochemical-thermal model for a Lithium-ion battery (LIB) based on porous electrode theory has been extended with contributions coming from exothermic side reactions based on an Arrhenius law to model abuse mechanisms, which could lead to a thermal runaway. These extensions have been modeled with a constant fuel model and for specified current profiles and exterior temperature profiles to simulate cell cycling under adiabatic conditions or an oven test repectively. The model has been implemented into COMSOL Multiphysics® (version 5.2) using the *Battery and Fuel Cell* Module coupled to the *Heat Transfer in Solids* Module. For a cylindrical 18650 cell with a $LiCoO_2$ cathode the spatial overall mean cell temperature $\overline{T}$ during the time evolution of a thermal runaway has been computed. Moreover the different stages of the thermal runaway have been classified in the phase space $\mathcal{T}$, which is spanned by a $\overline{T}$, $d\overline{T}/dt$, $d^2\overline{T}/dt^2$-plot.

Keywords: Thermal runaway, Lithium-ion battery, electrochemical-thermal model, constant fuel model, Arrhenius law

1. Introduction

Lithium-ion batteries (LIB) have found a wide range of applications in the last three decades, like notebooks, cell phones, powertools or hybrid or fully electric vehicles. The thermal runaway of a single cell in a larger battery pack is the worst case scenario which must be avoided under all circumstances. Several exothermic reactions can occur as the inner cell temperature is increasing. If the heat generation is larger than the dissipated heat to the surroundings, this leads to heat accumulation in the cell and acceleration of the chemical reactions, which can end up in a thermal runaway if the point of no return has been overcome.

The standard multi-scale multidomain (MSMD) models developed in [1-4] cannot simulate accurately the phenomenon of thermal runaway. First attempts to overcome this disadvantage are reported in [5], where the heat equation is coupled with ordinary differential equations (ODEs), describing the temporal evolution of the concentration of the exothermic reactions based on an Arrhenius-type law. Spotnitz et al. [6] give a first partial differential equation (PDE) based modeling of the thermal runaway including reaction kinetics. In [7, 8] the electrochemical-thermal model is extended with reaction kinetics based on an ODE formulation.

The same approach as in [8] has been used in this work and has been implemented into COMSOL Multiphysics®. This work is organized as follows. In section 2 the thermal modelling is briefly described. In Section 2.1, the thermal model is formulated and all heat sources are identified. In the following subsections the corresponding mathematical models, that are related to these heat sources are given. In Section 2.2, the electrochemical heat source is modeled using the MSMD model of LIB [3], which is implemented in the *Battery and Fuel Cell* Module in COMSOL Multiphysics®. Section 2.3 is devoted to the exothermic kinetic reactions leading to a thermal runaway, which are given in terms of mathematical combustion theory [9]. In Section 3 the implementation and the simulation using COMSOL Multiphysics® are described. Finally in section 4 simulation results for an oven test and simple electrical current loads are shown. Moreover the different stages of the thermal runaway have been classified.

2. Thermal modeling of Lithium-ion batteries

To model the thermal behavior of LIB the main focus is the consideration of a single cell. It is assumed that the interior of the cell is separated from the environmental air due to the battery can, so the cell can be considered as a closed system. Under general working conditions, LIB are exposed to an electrical and/or a thermal

load. As consequence, heat is generated inside the cell due to several electrochemical and chemical processes. If the heat generation inside the cell is smaller than the ability of the cell to dissipate heat to the environment, the cell is in a thermally stable state. If more heat is generated in the cell than can be dissipated to the environment the cell is in a thermally unstable state. The worst case scenario in this second case is the occurrence of a thermal runaway. The critical aspect in the case of a thermal runaway is its relation to the energy conservation. With the help of the energy conservation, one is able to describe thermal characteristics like heat generation and heat dissipation.

2.1 The energy conservation

If there is no heat convection inside the LIB, the general equation for the energy conservation can be derived from Fourier's law as initial boundary problem [9] with the parabolic differential equation:

$$\rho c_p \frac{\partial T}{\partial t}(\mathbf{x}, t) \kappa \Delta T(\mathbf{x}, t) + Q_{gen}(\mathbf{x}, t) \quad (1)$$

for the temperature $T : (\mathbf{x}, t) \in \Omega \times \mathbb{R}+ \mapsto \mathbb{R}$ of the cell in K. The corresponding initial and boundary conditions are:

$$T(\mathbf{x}, 0) = T(\mathbf{x}), \ \forall \ \mathbf{x} \in \overline{\Omega}, \quad (2)$$

$$\mathbf{n} \cdot (\kappa \nabla T) = -h(T - T_{env}) - \varepsilon \sigma(T_4 - T_{env}^4),$$
$$\forall \mathbf{x} \in \partial \Omega \quad (3)$$

In this framework $\mathbf{x} \in \overline{\Omega} \subset \mathbb{R}^3$ is an spatial interior or surface point of the cell and $t \in \mathbb{R}^+ := \{t \in \mathbb{R}, \ t \geq 0\}$ is the time. T_{env} denotes the environmental temperature, T_0 is the initial temperature profile inside the cell at $t = 0$ s. It is assumed, that the initial temperature at the boundary of the cell coincides with the environmental temperature at $t = 0$ s. Ω denotes the interior of the battery cell, $\partial \Omega$ represents the boundary of the cell and the closure $\overline{\Omega} = \Omega \cup \partial \Omega$ is the complete cell. Furthermore $\mathbf{n} \in \mathbb{R}^3$ is the outward pointing normal vector, h is the heat transfer coefficient, ε the emissivity, σ the Stefan-Boltzmann constant, ρ the density of the cell, c_p the heat capacity and κ the thermal conductivity. The solution of equation (1) describes the temperature distribution inside the cell for times $t > 0$ and all spatial points $\mathbf{x} \in \Omega$.

Equation (2) represents the given initial distribution of the temperature in the LIB at $t = 0$s. Finally equation (3) is the heat dissipation to the environment. The first term on the right hand side of equation (3) is the heat dissipation due to convection, while the second term describes the heat dissipation due to radiation. In the inhomogeneity Q_{gen} different heat sources are included. These contributions are coming from the heat generated by reversible and irreversible thermodynamic effects, which are represented by the electrochemical heat source $Q_{el-chem}$ and from exothermic kinetic side reactions $Q_{exotherm}$:

$$Q_{gen}(\mathbf{x}, t) = Q_{el-chem}(\mathbf{x}, t) + Q_{exotherm}(\mathbf{x}, t). \quad (4)$$

Thus, for $Q_{exotherm}$ and $Q_{el-chem}$ in equation (4) additional mathematical models must be formulated.

2.1 Identifying the electrochemical heat sources

If a cell is exposed to an electric load I, heat will be generated inside the cell due to the reversible and irreversible processes in the cathode, anode and the electrolyte of the LIB. The total electrochemical heat source is then:

$$Q_{el-chem} = Q_{rev} + Q_{irrev} \quad (5)$$

$$Q_{rev} = I \cdot T \cdot \frac{dU_{eq}}{dT} \quad (6)$$

$$Q_{irrev} = I(U - U_{eq}) \quad (7)$$

The critical variables in the electrochemical heat source are the equilibrium voltage U_{eq} and the derivation of the equilibrium voltage with respect to the temperature $\partial U_{eq}/\partial T$. Due to their porous structure the cathode and anode consist of the solid phase and a liquid phase filled with the electrolyte and a model based on the porous electrode model [10] has to be applied, which represents a multi-scale multi-domain approach (MSMD). Such an approach takes the physical and geometrical structure of the LIB on the different length scales and different geometrical domains into account. Charge transfer kinetics have to be solved on the electrode-electrolyte interface. The transport of the Li-ions is modeled with a diffusion mechanism and the migration and diffusion of the Li-ions through the liquid electrolyte can be evaluated. The charge balances in the solid cathode and anode as well as the

liquid electrolyte are also resolved in the corresponding matrices. To determine the electrochemical heat sources one has to apply the spatial averaging theorem to the corresponding current densities and heat fluxes on each domain level. A detailed survey can be found in [11] and the references therein.

2.3 Modeling the thermal runaway and exothermic heat sources

Exothermic reaction kinetics are closely related to thermal abuse mechanisms. Several exothermic chemical reactions can occur inside a cell as the temperature rises. This may generate heat that accumulates inside the cell and accelerates the chemical reaction between the cell components, if the heat generation rate exceeds the dissipation rate to the surroundings. External conditions for a temperature rise can be external heating, over-charging or over-discharging, high current charging, nail penetration, external short or others. In these cases a thermal runaway can occur in consequence with leakage, smoke, gas venting, flames etc., which leads to the destruction of the cells.

In detail the heat source in the corresponding heat equation is extended with various exothermic reactions, for example at the surface-electrolyte interface at temperatures in the interval $T \in [T_1, T_2]$, reactions between anode resp. cathode and the electrolyte between temperatures in the interval $T \in [T_3, T_4]$ and the destruction of the electrolyte above the temperature $T > T_5$, where $T_1 < T_2 < T_3 < T_4 < T_5$.

Several authors have given models to describe abuse behavior and thermal runaway. To describe the thermal runaway of a LIB one has to identify the main exothermic chemical reactions. Following [8, 12, 13] the general mechanism, that leads to a thermal runaway can be described with respect to rising temperature in four main stages as follows:

(1) SEI decomposition reaction: At $T > T_1$ the solid-electrolyte interface (SEI) will decompose in an exothermic reaction $\Rightarrow$ heat source Q_{sei}.

(2) Negative solvent reaction: At $T > T_2$ an exothermic reaction between the intercalated Li-ions and the electrolyte will start $\Rightarrow$ heat source Q_{ne}.

(3) Positive solvent reaction: For $T > T_3$ an exothermic reaction between the positive material and the electrolyte takes place under the evolution of oxygen inside the cell $\Rightarrow$ heat source Q_{pe}.

(4) Electrolyte decomposition: In a final exothermic reaction the electrolyte will decompose at $T > T_4$ $\Rightarrow$ heat source Q_{ele}.

For the exothermic heat source one assumes that the n independent exothermic reactions which occur in the LIB are governed by simple Arrhenius laws. Then the exothermic heat source is given as:

$$Q_{exotherm}(\mathbf{x}, t) = \sum_{i=1}^{n} Q_i(\mathbf{x}, t) \qquad (8)$$

with

$$Q_i(\mathbf{x}, t) = c_i(\mathbf{x}, t) q_i A_i \exp\left(-\frac{E_{a,i}}{RT(\mathbf{x}, t)}\right) \quad (9)$$

where $c_i(\mathbf{x}, t)$ is the dimensionless concentration, q_i is the reaction enthalpy in J g^{-1}, A_i is the frequency factor in $1/s$, $E_{a,i}$ is the activation energy in J mol^{-1} and R is the universal gas constant. For simulations in the next section, it is assumed that the concentration $c_i(\mathbf{x}, t)$ is constant. In this so-called *constant fuel model* all time-spatial dynamics of the concentrations are neglected. The exothermic heat sources defined in equation (9) are thus only dependent on the temperature T, i.e. for $i \in \{sei, pe, ne, ele\}$

$$Q_i(\mathbf{x}, t) = c_{i0} q_i A_i \exp\left(-\frac{E_{a,i}}{RT(\mathbf{x}, t)}\right) \qquad (10)$$

3. Use of COMSOL Multiphysics®

The mathematical model described in the last section represents a simple multi-scale multi-domain approach, which has been implemented in the *Battery and Fuel Cell Module* of *COMSOL Multiphysics*. For the simulations presented next, a cylindrical 18650 cell with LiCoO$_2$ chemistry was chosen and an axial-symmetric pseudo-2D model was implemented. From the material database in *COMSOL*

Multiphysics a Li_xC_6 anode, a Li_xCoO_2 cathode and as electrolyte 1:1 EC : DEC with a $LiPF_6$ salt is used. The internal spirally wound geometry is not resolved. From the reaction-diffusion system of the exothermic reactions inside the LIB only the additional heat sources are used to extend the heat transport equation with additional heat sources (constant fuel model). The main physical parameters of the simulations can be found in [11].

For the simulations two physical relevant cases under adiabatic conditions, i.e. the convective heat transfer coefficient h vanishes, have been considered:

(a) Oven test: In this case the LIB will be heated from exterior with a certain heating rate (Figure 1(a)).

(b) Electric load: The LIB will be heated from the interior due to the active battery material with respect to the applied electric current (Figure 1 (b)).
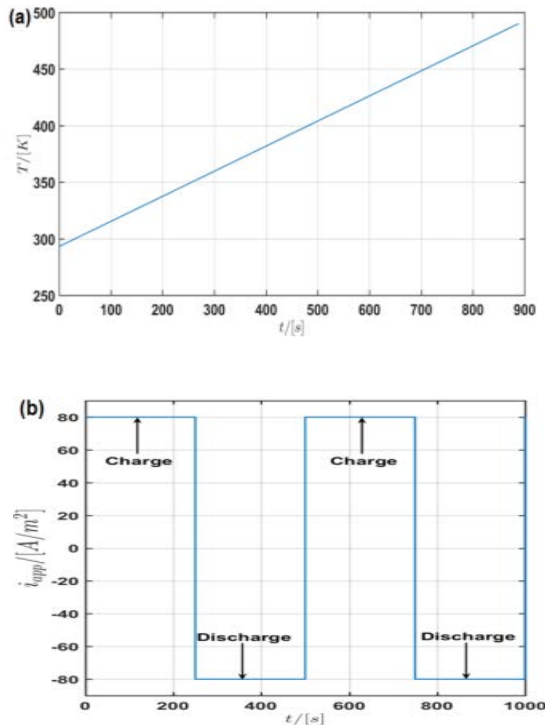

Figure 1. (a): Oven test with a heating rate of ($d\overline{T}/dt$ = 5K/min). (b): Cycling with a periodic electrical current load ($T_{cycling}$ = 500 s, $\hat{I}_{app}$ = 80 A/m²).

The simulations were performed in COMSOL Multiphysics Version 5.2. For the time integration a backward differentiation formula (BDF) integration scheme is chosen with a minimum order of 1 and a maximum order of 5 using a variable step size with a maximum time step of 1s and an absolute tolerance of 0.001. Since the spatial discretisation is based on the Finite Element Method (FEM) an adaptive spatial discretisation in the three models of the particle domain, the electrode and the cell domain is used. The model of the particle domain is solved automatically in the *Battery and Fuel Cell* Module. Therefore only a spatial discretisation for the electrode domain and the cell domain is needed. The electrode domain is one-dimensional and the cell domain is modeled due to symmetry reasons in the angular direction of a cylindrical cell as two-dimensional. In the electrode domain, the maximum element size in the discretisation is chosen as 1 µm. And in total, the discretisation contains 168 elements. For the one-dimensional finite element discretisation in the electrode domain quadratic basis functions were chosen. In the cell domain the spatial discretisation is performed in the $r - z$-plane using 2266 triangular elements with the element size in the interval $[3.9 \cdot 10^{-4}, 8.45 \cdot 10^{-2}]$m and quadratic basis functions.

To simulate an oven test, an additional boundary condition is implemented in the model, which describes the increasing environmental temperature during heating by a surface heat source Q_{surf}, with Q_{surf} = 1809 W/m². This value is equivalent to a constant heating rate of 5K/min.

4. Simulation Results and Discussion

To classify the different stages of a thermal runaway in the phase-space $\mathcal{T}$ the overall spatial mean cell temperature $\overline{T}$, and their first $d\overline{T}/dt$ and second $d^2\overline{T}/dt^2$ time derivative are considered.

$$\overline{T}(t) := \frac{1}{V} \int_V T(\mathbf{x}, t) dx \qquad (11)$$

The time evolution of the overall mean cell temperature towards the thermal runaway is given in Figure 2. In the Figure 3 the two-dimensional projections of the phase-space $\mathcal{T}$ for the oven trial (I) and the electric load (II) are

shown. The horizontal and vertical dashed lines coincide with critical heating rates $d\overline{T}/dt$ and temperatures $\overline{T}$ as described in [13]. From Figure 3 one can identify three zones during the rise of the temperature $\overline{T}$ towards the thermal runaway depending on both cases. In general one can discriminate between:

- Zone 1: Below $\overline{T} \approx 400$ K the heating rate $d\overline{T}/dt$ is bounded below a threshold $d\overline{T}/dt|_{thres,1}$ at a low level at a nearly constant rate for the oven trial (Figure 3 (I)(a)) and slightly increasing for the electric current profile (Figure 3 (II)(a)). In Figure 3 (b) the corresponding evolution of $d^2\overline{T}/dt^2$ with respect to T is given. Furthermore one can see that below temperatures of $\overline{T} \approx 360$ K $d^2\overline{T}/dt^2$ is decreasing and becomes negative (gap in the plot (I) (b)). Above $\overline{T} \approx 360$ K $d^2\overline{T}/dt^2$ is increasing and positive. For the case of electric cycling (Figure 3 (II)(b)) below $\overline{T} \approx 400$ K one can see that during a charging pulse the heating rate is increasing, while for a discharging pulse the heating rate is decreasing and becomes negative (gap in the plot). This can be seen in the left area of the Figure 3, (I)/(II)(c) as well.

- Zone 2: In Figure 3 (I)(a) for the oven-trial the heating rate is rising above $\overline{T} \approx 400$ K while the overall mean cell temperature is rising, but stays bounded below a threshold $d\overline{T}/dt|_{thres,2}$. More precise the increase in the heating rate starts already at temperatures $\overline{T} \approx 360$ K (Figure 3 (I)(b)). For the electric current profile a similar behavior is shown in the Figure 3 (II) above $\overline{T} \approx 400$ K which is perturbed by the jumps of the current profile. The corresponding relationship between $d\overline{T}/dt$ and $d^2\overline{T}/dt^2$ is shown in the middle area of the Figure 3, (I)/(II)(c).
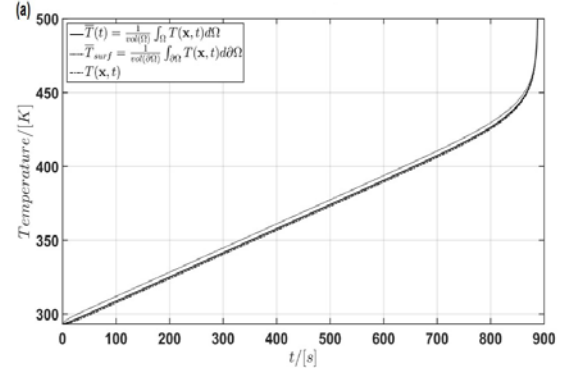

Figure 2. Thermal runaway during an oven test.

- Zone 3: Finally for temperatures $\overline{T} \geq 435$ K the heating rate $d\overline{T}/dt$ as function of the overall mean cell temperature $\overline{T}$ shows a linear increase in the semi-logarithmic plot of the Figure 3,(I)/(II)(a). This corresponds to an exponential dependence of $d\overline{T}/dt$ with respect to $\overline{T}$ i.e.

$$\frac{d\overline{T}}{dt} = a \cdot \exp(b \cdot \overline{T}), \overline{T} \geq T_0 \qquad (12)$$

where T_0 is the lower bound, where this dependency is valid, and a, b are some constants. A similar behavior can be found for $d^2\overline{T}/dt^2$ in the Figure 3, (I)/(II) (b). In general one can show by induction that the n-th time derivative of the overall mean cell temperature shows an exponential growth behavior with respect to $\overline{T}$:

$$\frac{d^n\overline{T}}{dt^n} = a_n \cdot \exp(b_n \cdot \overline{T}), \overline{T} \geq T_0, n \geq 1 \quad (13)$$

with a_n, b_n some constants. This is the region where the thermal runaway starts, which is equivalent with a blow-up in the temperature curve and the time derivatives of arbitrary order. The double-logarithmic plot in the Figure 3, (I)/(II)(c) shows a linear dependency between $d^2\overline{T}/dt^2$ and $d\overline{T}/dt$ in the right area of the plots. Again by induction one can show that the n-th time derivative $n \geq 2$ of the overall mean cell temperature shows a linear behavior with respect to the heating rate $d\overline{T}/dt$, i.e.

$$\frac{d^2\overline{T}}{dt^2} = A \cdot \frac{dT}{dt} + B, \overline{T} \geq \overline{T}_0 \quad (14)$$
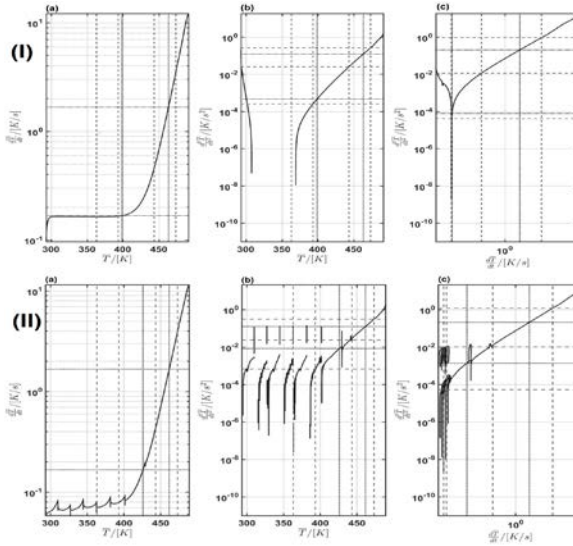
where A, B are some constants.

Figure 3. Two-dimensional projections of the phase-space $\mathcal{T}$ (a) $\overline{T} - d\overline{T}/dt$ -trajectory, (b) $\overline{T} - d^2\overline{T}/dt^2$-trajectory, (c) $d\overline{T}/dt - d^2\overline{T}/dt^2$-trajectory. (I) oven test, (II) electric load.

5. Conclusion

Since we have some electrochemical and some exothermic heat sources in the thermal model, the results from the last section have the following physical meaning (Figure 4):

- Zone 1: In this zone the electrochemical heat sources represented by the reversible and irreversible part are dominant. The exothermic heat sources can be neglected. This zone corresponds to a thermal stable state of the LIB.

- Zone 2: Due to the rise in the temperature the exothermic heat sources start to become more active. This zone can be considered as a transient zone on the way from a thermal stable to a thermal unstable state of the cell

- Zone 3: In this zone the exothermic heat sources are dominant and the electrochemical heat sources can be neglected. This zone corresponds to a thermal unstable state of the LIB which represents the thermal runaway.
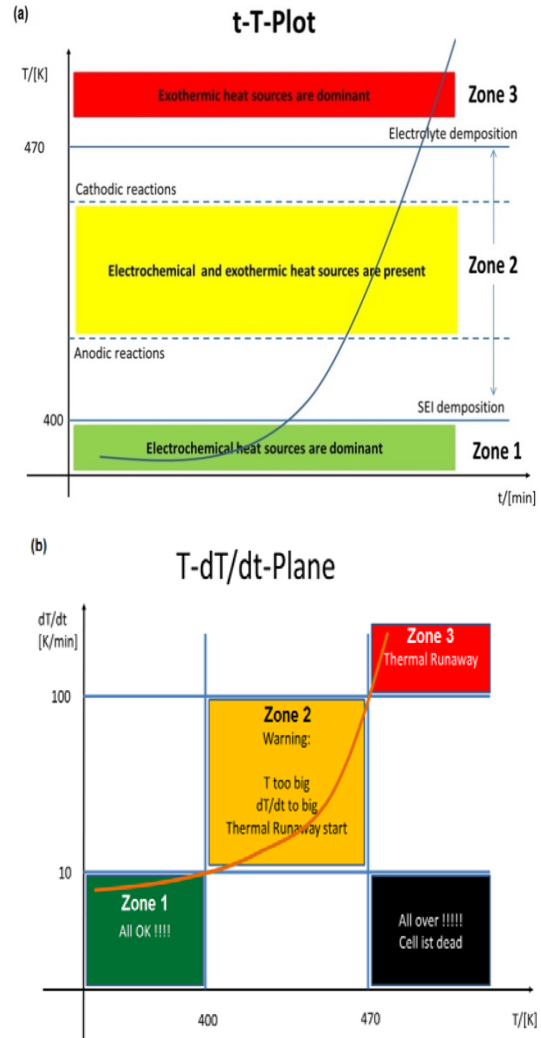

Figure 4. Thermal Runaway classification: (a) In the temperature vs. time plot. (b) In the temperature rate vs. temperature plot.

6. References

1. W.B. Gu, C.Y. Wang, *Thermal-Electrochemical Modeling of Battery Systems*, J. Electrochem. Soc. **147**, 2910–2922 (2000).

2. C.Y. Wang, V. Srinivasan, *Computational battery dynamics - electrochemical/thermal coupled modeling and multi-scale modeling*. J. Power Sources **110**, 364–376 (2002).

3. L. Cai, R.E. White, *Mathematical modeling of lithium ion battery with thermal effects in COMSOL Inc. Multiphysics (MP) software*, J. Power Sources **196**, 5985–5989 (2011).

4. K.J. Lee, K. Smith, A. Pesaran, G.H. Kim, *Three dimensional thermal-, electrical, and electrochemical-coupled model for cylindrical wound large format lithium-ion batteries*, J. Power Sources **241**, 20–32 (2013).

5. T.D. Hatchard, D.D. MacNeil, A. Basu, J.R. Dahn, *Thermal Model of Cylindrical and Prismatic Lithium-Ion Cells*, J. Electrochem. Soc. **148** A755–A761 (2001).

6. R. Spotnitz, J. Franklin, *Abuse behavior of high-power, lithium-ion cells*, J. Power Sources **113**, 81–100 (2003).

7. G.H. Kim, A. Pesaran, R. Spotnitz, *A three-dimensional thermal abuse model for lithium-ion cells*, J. Power Sources **170**, 476–489 (2007).

8. P. Peng, Y. Sun, F. Jiang, *Thermal analyses of LiCoO2 lithium-ion battery during oven tests*, Heat Mass Transf. **50**, 1405–1416 (2014).

9. J. Bebernes, D.Eberly, *Mathematical Problems from Combustion Theory*, Applied Mathematical Sciences Volume 83, Springer, Berlin, Germany, 1989.

10. J. Newman, W. Tiedemann, *Porous-Electrode Theory with Battery Applications*, AIChE Journal, **21**, 25–41 (1975).

11. A. Melcher, C. Ziebert, M. Rohde, B. Lei, H.J. Seifert, *Modeling and Simulation of the Thermal Runaway Behavior of Cylindrical Li-Ion Cells - Computing of Critical Parameters*, Energies **9** 292 (2016).

12. T.D. Hatchard, D.D. MacNeil, A. Basu, J.R. Dahn, *Thermal Model of Cylindrical and Prismatic Lithium-Ion Cells*, J. Electrochem. Soc. **148** A755-A761 (2001).

13. D.P. Abraham, E.P. Roth, R. Kostecki, K. McCarthy, S. MacLaren, D.H. Doughty, *Diagnostic examination of thermally abused high-power Lithium-ion cells*, J. Power Sources **161** 648-657 (2006).

7. Acknowledgements